Integrated Composite Stiffener Structure (ICoSS) Concept for Planetary Entry Vehicles

Sotiris Kellas[1]
NASA Langley Research Center, Hampton, VA 23681

Results from the design, manufacturing, and testing of a lightweight Integrated Composite Stiffened Structure (ICoSS) concept, intended for multi-mission planetary entry vehicles are presented. Tests from both component and full-scale tests for a typical Earth Entry Vehicle forward shell manufactured using the ICoSS concept are presented and advantages of the concept for the particular application of passive Earth Entry Vehicles over other structural concepts are discussed.

I. Introduction

In the late 1990s researchers at NASA Langley began investigating the feasibility of a passive Earth Entry Vehicle (EEV)[1]. By eliminating all active systems and relying solely on passive energy absorbers for load attenuation at landing, the passive EEV could meet a much higher level of reliability when compared with conventional entry vehicles[2]. In the mid 2000's work was performed to develop a Multi-Mission Earth-Entry Vehicle concept coined MMEV[3] accompanied later by a systems analysis for Planetary Entry tool[4].

The ICoSS is a natural extension of the earlier EEV work performed at NASA Langley with the main objective of providing off-the-shelf design tools for Entry Vehicles. In addition to offering a lightweight solution, the ICoSS concept offers structural optimization flexibility to meet evolving mission requirements without requiring re-tooling. Its fully integrated stiffeners are formed over lightweight Computer Numerical Control (CNC) machined closed foam core, which can be modified at any time during the design process. Therefore, stiffener geometry and layout can be optimized to meet evolving loads and environments without budget and schedule penalties. Perhaps the biggest advantage the ICoSS concept offers is uninterrupted load paths for both axial and shear loads across stiffener intersections.

The ICoSS concept is compatible with nearly all polymer composite manufacturing methods and/or fiber architectures. Four approximately 1.1m diameter forward shells have been designed, fabricated and tested to demonstrate some of the advantages that the concept has to offer.

The unique and challenging structural requirements for a passive EEV, which, in addition to launch and aerothermodynamic entry loads include high landing loads, make the ICoSS concept very attractive for this particular application.

II. Passive EEV Structural Requirements

In general, a conventional EEV structure is designed to handle launch and re-entry loads with re-entry typically being the most demanding condition, particularly for the forward shell which is subjected to the highest pressure and heat loads. Typically, the structural design is stiffness critical and actual deflection limits are dictated by the Thermal Protection System (TPS).

The main distinguishing feature between a passive and conventional EEV is the landing velocity. Lack of active systems to dissipate kinetic energy in the subsonic regime means that the passive EEV lands at a much higher velocity compared to a parachuted vehicle. Higher landing velocity introduces extra structural design challenges, which also depend on the choice of one of two broad methods for dissipating the impact energy. The first method is the one employed by the original passive-EEV[5] and it is referred to as the "Racecar" energy absorbing method. The second is the "Camera-Case" energy absorbing method. These two options typically represent the absolute opposite extremes in impact-load attenuation approach and are shown schematically in Figure 1.

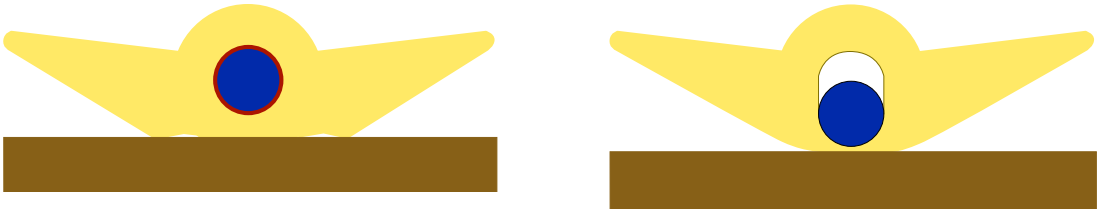

(a) “Racecar” (b) “Camera-Case”

Figure 1. Schematics of typical EEV cross-sections for the two bounding cases of energy absorbing methods shown at impact. The yellow area represents the vehicle and the blue circular area represents the payload. The brown area represents the ground.

Which method is ultimately chosen depends on mission requirements but the important point is that the chosen energy absorbing method defines additional structural design requirements for the entry vehicle and the forward shell in particular.

In the case of the racecar option, it is normally assumed that the landing surface is hard and all energy has to be absorbed by crushing of the forward shell – Just like a racecar, any structure that surrounds a reinforced-cockpit can be thought of as frangible and it is therefore relied on for energy absorption during a crash. To the contrary, the camera-case method requires the outer shell to be stiff and non-frangible and all impact energy is absorbed by deformation of internally contained energy absorbing structure/material. Each method has advantages and disadvantages.

The racecar approach is more often suited to high-energy impacts and/or when the ground is hard. The advantage of this approach is that the vehicle structure becomes multipurpose and could offer some mass benefits. Relatively simpler to achieve good coupling between the payload and the vehicle is another advantage offered by the racecar method. A major disadvantage is the challenge of achieving a fine balance between a stiff enough forward shell structure to adequately support the TPS during launch and atmospheric entry, and also to crush efficiently during impact. Another challenge associated with the racecar method is the necessity for system-level analysis and verification.

While the camera-case option is typically better suited to lower energy impacts, it can be utilized in some higher energy applications provided that a significant portion of the kinetic energy can be dissipated by soil penetration. The main advantage of this method, assuming the vehicle outer shell remains sufficiently intact during impact, is that the energy absorbing response can be decoupled from the rest of the vehicle and hence the energy absorber can be verified independently. A major disadvantage/complexity of this design is associated with the way the payload is attached to the energy absorber and the fact that secondary impacts may prove detrimental should the payload become detached during the primary impact event. In reality, no mater which method is chosen the final outcome will be some combination of the two.

Given the added complexity of high-velocity impact, the ICoSS concept is well suited to the passive EEV applications and can be tailored either towards the “racecar” or the “camera-case” design approaches.

III. ICoSS Structural Concept Description

The ICoSS concept provides a cost-effective and lightweight structural solution that takes full advantage of composite material forms and manufacturing processes to minimize cost and maximize structural performance while offering design flexibility without the requirement for intricate retooling typically required for grid stiffened structures[6]. In addition to EEV applications, the concept is expected to have a significant impact in the design/manufacturing of any small-production run structures.

Features that make ICoSS unique include the co-cured stiffener junctions, which offer uninterrupted load paths across intersections, and fully customizable stiffener architecture. Stiffener geometry and layout is defined by the machined foam core and therefore modifications to the stiffener architecture, including stiffener geometry, stiffness, and intersection angle modifications, can be accomplished without the need for retooling. Moreover, the ICoSS concept is compatible with a variety of material forms and manufacturing processes and has the capability of taking full advantage of what fiber reinforced composites have to offer.

Figure 2 describes the three basic elements used in the construction of a typical EEV forward shell. A tool surface (not shown in Figure 2) typically is required to define the shell Outer Mold Line (OML). Following the placement of the OML plies on the tool, a CNC machined core that defines a network of stiffeners is positioned over

the OML plies. The core, which is often closed cell foam, contains an appropriate amount of fiber reinforcement to meet the shells global stiffness requirements. The integrating plies follow next before the entire assembly is co-cured. Photographs of a prototype EEV forward shell, fabricated using the ICoSS concept are shown in Figure 3.

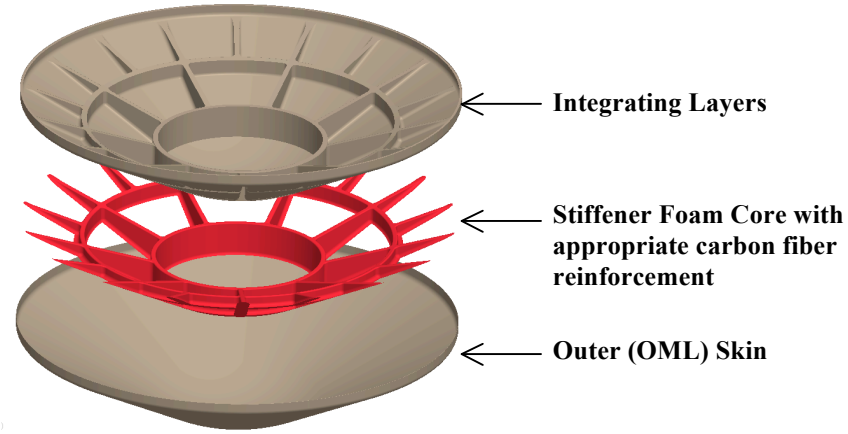

Figure 2. Schematic of the ICoSS Structural Concept

Figure 3. Prototype EEV forward shell. Pocket is defined as the area contained between two radial and two circumferential stiffeners

Available options for optimizing the global stiffness of the shell include stiffness geometry, stiffener layout, and/or amount and orientation of fiber reinforcement. For a given stiffener layout, local stiffness optimization in areas between stiffeners (called pockets) can be achieved through fiber orientation in the OML skin, thickness of the pocket skin and/or added core in the pockets to produce a sandwich construction.

IV Typical EEV Forward Shell Application

A. ICoSS Advantages For EEVs

Because the network of stiffeners and/or fiber reinforcement that control the global stiffness of the shell can be modified relatively easily, the ICoSS concept can be tailored to meet evolving vehicle requirements such as TPS type and/or TPS thickness, which can lead to mass savings. In the case of the passive EEV, the ICoSS concept can be customized for either the "racecar" or "camera case" energy absorbing methods by simply manipulating the stiffener geometry and/or reinforcement to produce the desired features without a significant mass and/or program schedule penalty. The stiffeners and stiffener intersections also offer options for hard points to react loads from launch and/or parachute deployment for an active EEV, and offer ample choices for system integration and/or internal mounting points for instrumentation and other hardware. For example, the inner circular frame (shown in Figure 3) can be used to secure the energy absorbing structure for a passive EEV. Because of the inability of the sandwich construction to react out-of-plane loads such integration would have required a significant amount of redesign, fabrication complexity, and mass for a sandwich forward shell.

Local stiffness (pocket areas) is typically controlled by the stiffener spacing, fiber orientation, and the total number of plies within the pockets. Another option for improving local stiffness is to add core in the pockets to essentially generate a sandwich construction. While this option may be mass efficient in theory, it adds complexity to the manufacturing process. Depending on requirements, the core can occupy the entire pocket area or a part of it.

B. ICoSS Manufacturing Development

Several forward EEV shells were fabricated using the same mold and stiffener geometry. The main objectives were to assess the degree of difficulty associated with (a) various options of applying fiber reinforcement to the stiffener core and (b) the addition of core in the pockets of the shell. While options and/or methods for reinforcing the foam core are not discussed in this paper, the effect of core in the pockets will be addressed.

The shell consisted of a spherical nose that transitioned to a conical surface as shown in Figure 3. One prototype and three Manufacturing Development Units (MDU) were fabricated from the same mold that defined the OML shape of the shells. Other common parameters to all shells were the stiffener shape and the stiffener layout. Parameters that were different included stiffener foam-core type, stiffener foam-core reinforcement, and introduction of thin foam-core in the pockets of one of the shells.

All MDUs were modeled using Pro-E Computer Aided Design (CAD) software and built using graphite woven fabric in conjunction with wet layup and room temperature curing processes. While relatively inexpensive materials and layup techniques were utilized, the processes were modified as much as practically possible to simulate more advanced fabrication techniques. For example, the shape of all integrating plies was optimized using "Fibersim" software. Each integrating ply was then cut from dry-fabric using a CNC ply cutting machine for speed and accuracy. This allowed for relatively better control of fiber-reinforcement mass and uniformity across the shell and emulated a technique that is typically used with pre-impregnated materials.

Challenges associated with wet layup such as difficulty in maintaining desired fiber orientations, lack of fiber-volume-fraction control and good consolidation, introduced extra complexity to the test/analysis correlations, but overall, this method proved adequate in meeting the manufacturing development and test objectives of the project.

In this paper, particular emphasis will be placed on the comparisons between two shells that were identical in all aspects of fabrication and fiber orientation except for added foam core in the pockets of one of the shells.

CAD mass estimates for the two shells were compared against the as-built mass. Inputs to the CAD mass included material density measurements from flat panels fabricated in the same way as the ICoSS shells. Compared to the CAD mass the as-built mass was 3.9% and 7.0% greater for plain and sandwich-pocket shell, respectively. Moreover, the as-built shell with the sandwich pockets was 9.0% heavier than the shell with the plain pockets. The greater than predicted mass difference between the shells is attributed to extra resin absorbed by the rough surface of the foam-core and resin rich regions around the perimeter of the pocket due to the increased geometric complexity. Given the wet layup technique in conjunction with limited (vacuum) pressure, the as-built mass numbers were well within expectations. It is anticipated that introduction of autoclave processing in conjunction with pre-impregnated materials can decrease the mass difference between the plain and sandwich pocket shells and bring it closer to the CAD estimated difference of 5.9%. It is also worth mentioning that the foam core occupied nearly the entire surface of the pockets and no attempt was made to optimize the thickness and/or area of the core. Clearly, proper sizing of the core area and facesheets within the pocket areas should lead to significant mass savings.

C. ICoSS Shell Testing

All MDUs were pressure tested to a predetermined maximum load that a given shell could sustain without failure. Maximum load capability was estimated for each shell using Finite Element Analysis. The three MDUs were successfully pressure tested without failure and/or permanent deformation.

Two of the shells were subsequently dissected to obtain individual stiffeners and pocket skin coupons. These were tested to provide as-built mechanical properties to improve the test/analyses correlations and to study the response of individual stiffeners. Pressure test results are presented for two shells and individual stiffener test results are presented for a single shell.

1. Full-Scale Pressure Test

The objective of the full-scale test was to assess shell-stiffness uniformity for the various fabrication options and to provide data to validate the analytical models that could be used for future parametric and/or structural optimization studies. Achieving a given ultimate load and/or minimum displacement was not a goal.

The goal of the pressure test was to achieve a known loading and boundary condition rather than simulate flight loads. Therefore, a simple technique was used to apply uniform external pressure to the shell. The shells were potted in a 13 mm deep slot machined in a stiff aluminum annular frame. The aluminum frame also contained a pressure-

gage, and a vacuum port as shown in the schematic of Figure 4(a). A pressure transducer port, not shown in Figure 4(a) was also machined in the aluminum frame. The potted shell and frame were vacuum-sealed to a heavy metal surface-table and uniform external pressure was achieved by generating vacuum inside the shell. Eliminating a vacuum bag and/or any other means of applying pressure directly on the OML of the shell allowed for a speckled pattern, shown in Figure 4(b), to be applied and photogrammetry to be used for precise full-field deformation measurements.

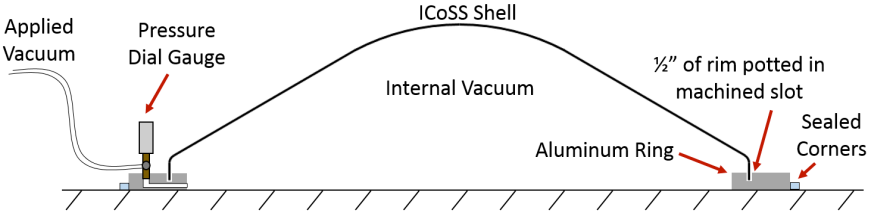

(a) Schematic of the test set-up

(b) Photograph of speckled shell in test frame

Figure 4. Pressure test set-up

Photogrammetric measurements were checked against laser measurements at predetermined points on the shell during preliminary tests as well as at given checkpoints during the test. Shell full-field deformations were monitored in real time during loading and unloading of the shell to verify that failure did not occur and that no residual deformation remained after the load was removed.

Pressure test results are presented for two shells which as mentioned above from a fabrication point of view, were identical except for the introduction of foam core in the pockets of one of the shells. Test results, in the form of vertical displacement of the shell apex as a function of applied pressure highlight (Figure 5) the similarity in the global displacement response for the two shells. Approximately 2.65 mm of maximum deflection was measured at the peak-applied pressure of 48.3 kPa (7.0 psi) for both shells. For clarity, only the loading portion from each test is plotted in Figure 5. It is worth mentioning that both shells had zero residual deflection when the applied pressure was removed. As anticipated, the test results confirmed that the global stiffness response of the shell is controlled primarily by the integrated stiffener architecture.

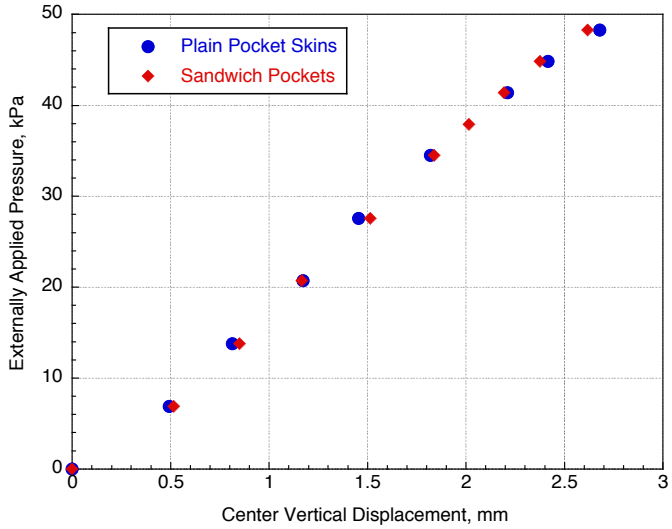

Figure 5. External pressure versus center shell deflections for a shell with and one without core in the pockets

While primarily the stiffeners control the global deflection response of the shell, the local pocket deflections are controlled, amongst other parameters, by the architecture of the pockets. The effect of pocket construction on the local displacement response is presented in Figure 6 in a side-by-side comparison of the full-field vertical deflections for the two shells at the same peak external pressure. Clearly, the shell with plain pockets exhibits local deformations in the center of the pockets, which are greater than the perimeter of the pockets. These localized deformations occur earlier in the outer row of pockets were the curvature in the OML skin is the lowest. In addition, one pocket in the inner row of pockets, identified by the white arrow in Figure 6(a), also shows relatively large vertical displacement. Closer examination of the entire data set revealed that this particular pocket underwent an elastic snap-through deformation just before the maximum pressure was reached.

Noticeably different, the shell with core in the pockets exhibits a much more uniform deformation with practically no relative deformations in the center of the pockets as shown in Figure 6(b).

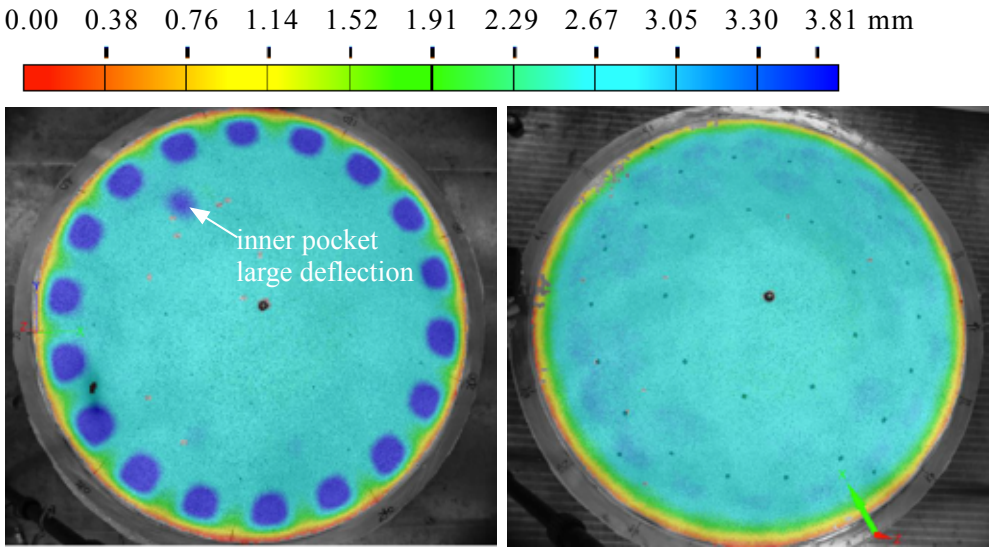

(a) Shell plain pockets (b) Shell with sandwich pockets

Figure 6. Full-field vertical displacements at peak applied pressure of 48.3 kPa (7.0 psi).

2. Component and coupon tests

Following the pressure test, the shell with plain pockets was dissected as shown in Figure 7(a). An individual radial stiffener being prepared for test is shown in Figure 7(b). In addition, to complete radial stiffener samples, two coupons (radial orientation) were removed from each pocket for as-built tensile strength and stiffness measurements. Each stiffener was tested in three point bend to evaluate uniformity/accuracy of the fabrication process and to provide additional data for test/analysis correlations.

The nine stiffener samples were as long as the conical section of the shell and contained a part of the OML skin as shown in figure 7(b). Therefore, any measured variations in strength and stiffness are the combined effect of the stiffener constituents as well as the fiber orientation accuracy of the OML skin. Each stiffener sample was loaded in an asymmetric three-point bend fashion. Load was applied through a ball bearing resting on a small aluminum block that was located over the cruciform junction as shown in Figure 7(b). The load orientation was such that to simulate a similar bending condition that the shell experiences under external pressure loads – OML skin in compression.

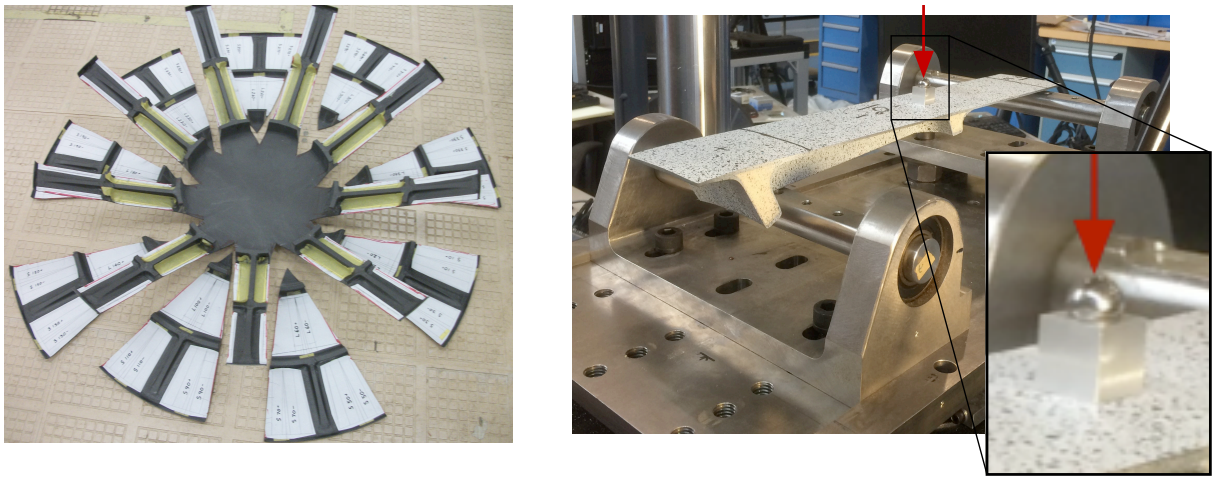

(a) Photo of dissected shell with all nine radial stiffeners still attached to the spherical section of the shell

(b) Radial stiffener shown on three-point-bend test fixture

Figure 7. Post-pressure test dissection of ICoSS shell into coupons and component samples

The main objectives of the stiffener tests were (a) assessment of stiffness and strength uniformity, and (b) assessment of the cruciform junction response. A summary of load deflection responses of all nine stiffeners is presented in Figure 8. Stiffness, for each frame, was determined by calculating the initial slope (linear best fit between 0.0 and 3.0mm) of the load/displacement response. The average stiffness for all nine frames was 14.3 kgf/mm with a coefficient of variation of 6.5%. The average strength was 133.4 kgf with a coefficient of variation of 7.9%. All stiffener samples failed on the tensile side and at approximately the same location as shown in Figure 9.

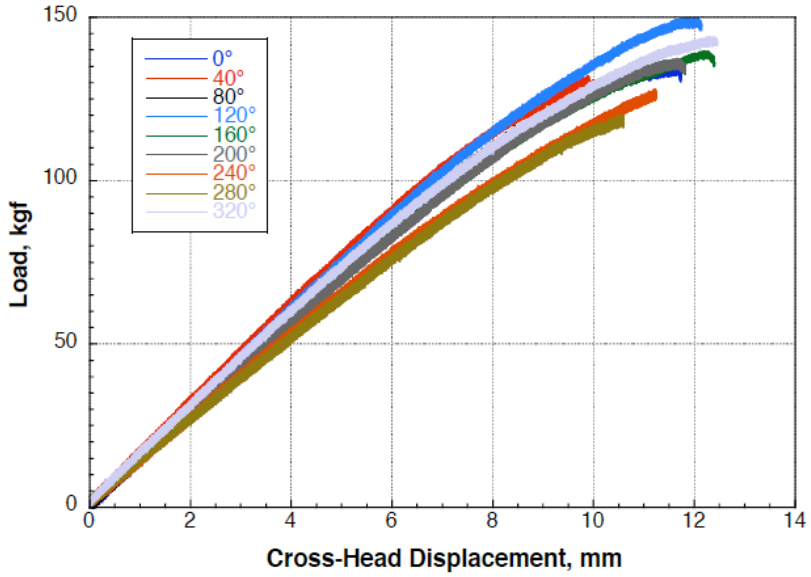

Figure 8. Three point bend responses for nine stiffener samples belonging to a single shell.

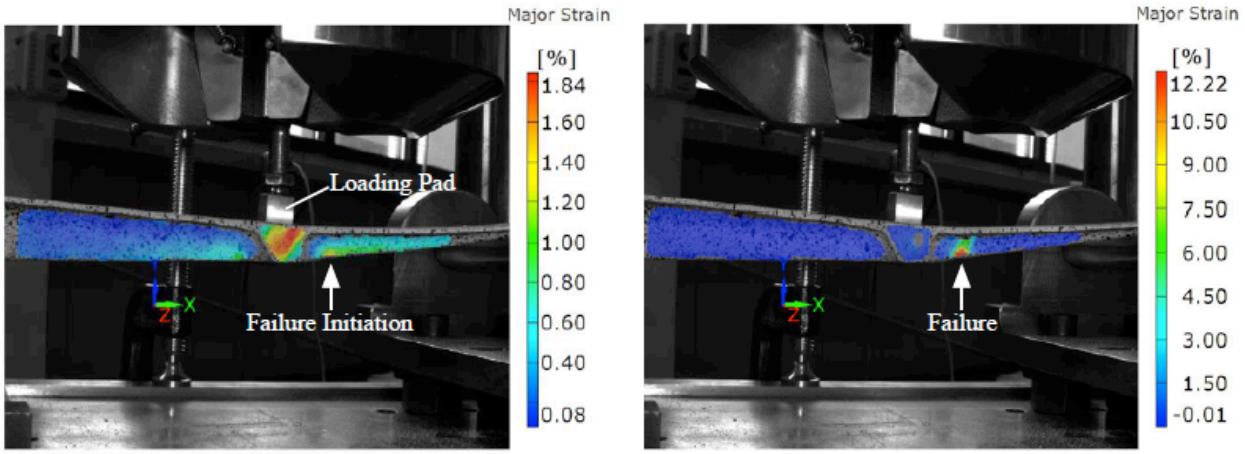

Figure 9. Photogrammetry images of full-field principal major strains for the 80° frame immediately before (left image) and after failure (right image).

V Summary and Conclusions

The Integrated Composite Stiffener Structural concept is a hybrid between composite grid stiffened structures[6] and a sandwich construction. As such it has the ability to take advantage of the uniform stiffness offered by the sandwich construction and/or the mass efficiency offered by the grid-stiffened concepts for large structures.

Which structural concept is best for a given application depends on many factors including shape of the structure, scale, loading, operating environment, fabrication, and operating cost. And while it is impossible for a single structural concept to meet every design requirement in an efficient manner, MDU fabrication and testing of the ICoSS shells highlighted some of the advantages that the concept has to offer for Earth Entry Vehicles and in particular the passive EEV where demanding landing loads eliminate options such as the sandwich construction which was used successfully in parachuted entry vehicles such as the Stardust[7].

Acknowledgments

The author would like to acknowledge contributions made by the following individuals: Mr Donald Smith of NASA LaRC for leading the fabrication of all ICoSS shells, and Dr. Justin Littell of NASA LaRC for performing the testing and photogrammetry data processing.

References

[1]Mitcheltree R. A., Kellas S., Dorsey J. T. Desai P. N, and Martin C. J., "A Passive Earth-Entry Capsule for Mars Sample Return," 7th AIAA/ASME Joint Thermophysics and Heat Transfer Conference, Paper 98-2851, Albuquerque NM, June 1998.

[2]Dornheim, Atkins K. L., Brownlee D. E., Duxbury T., Yen C. and Tsou P., "STARDUST: Discovery's Interstellar Dust and Cometary Sample Return Mission," Proceedings 1997 IEEE Aerospace Conference, Feb. 1997

[3]Maddock, R. W., "Sample Return Challenges Multi-Mission Earth Entry Vehicle Design Trade Space and Concept Development Strategy," 6th International Planetary Probe Workshop, Atlanta, GA, June 2008.

[4]Samareh, J. A., "A Multidisciplinary Tool for Systems Analysis of Planetary Entry, Descent, and Landing (SAPE)," NASA-TM-2009-215950

[5]Kellas S. and Mitcheltree R. A., "Energy Absorber Design, Fabrication and Testing for a Passive Earth Entry Vehicle", 43rd AIAAASME/ASCE/AHS/ASC/SDM, Denver CO, April 2002.

[6]Huybrechts S. M., Hahn S. E. and Meink T. E. "Grid Stiffened Structures: A Survey of Fabrication, Analysis and Design Methods," Proceedings of the *12Internation Conference on Composite Materials* (ICCM/12), Paris, France, 1999.

[7]Willcockson W. H., "Stardust Sample Return Capsule Design Experience," Journal of Spacecraft and Rockets Vol. 36, No. 3, May-June 1999